Organic Two-Layer Light-Emitting Diodes Based on High-T_g Hole-Transporting Polymers with Different Redox Potentials

Erika Bellmann,[†] Sean E. Shaheen,[‡] Robert H. Grubbs,*[,†] Seth R. Marder,[§] Bernard Kippelen,[‡] and Nasser Peyghambarian[‡]

Arnold and Mabel Beckman Laboratories of Chemical Synthesis, Division of Chemistry and Chemical Engineering, California Institute of Technology, Pasadena, California 91125, Optical Sciences Center, University of Arizona, Tucson, Arizona 85721, and Department of Chemistry, University of Arizona, Tucson, Arizona 85721

Received September 8, 1998. Revised Manuscript Received November 13, 1998

A series of soluble arylamine-based hole-transporting polymers with glass transition temperatures in the range of 130−150 °C have been synthesized. The synthetic methodology allows facile substitution of the aryl groups on the amine with electron-withdrawing and electron-donating moieties, which permits tuning of the redox potential of the polymer. These polymers have been used as hole-transport layers (HTLs) in two-layer light-emitting diodes ITO/HTL/Alq/Mg [ITO = indium tin oxide, Alq = tris(8-quinolinato)aluminum]. The maximum external quantum efficiency of the device increases if the redox potential of the HTL is increased to facilitate reduction of the positive charge carriers at the HTL/Alq interface. A fluorinated hole-transport polymer with a relatively large redox potential (390 mV vs ferrocenium/ferrocene) yielded the device with the highest external quantum efficiency of 1.25% photons/e^-. The device stability, however, follows the opposite trend. The device with the most electron-rich HTL exhibited the best performance after prolonged usage.

Introduction

Many organic light-emitting diodes (LEDs) are two-layer devices with a hole-transporting layer (HTL) between the anode [most commonly indium tin oxide (ITO)] and the electroluminescent layer (EL) (Figure 1). The hole-transporting material traps the electrons inside the EL but allows hole injection into the EL. This facilitates exciton formation inside the EL or at the HTL/EL interface, consequently improving the overall device characteristics. Three key properties of the hole-transport material impact the performance of the device: (i) the hole mobility within the material, (ii) its redox potential, and (iii) its thermal/electrochemical stability.

Hole mobilities in organic materials have been widely studied,[1−5] and they have been shown to correlate with device performance.[6] The redox potential determines how easily the material is oxidized at the anode/HTL interface (Figure 1, reaction 1), or how easily its radical cation is reduced at the HTL/EL interface (Figure 1, reactions 2 and 3). Relatively electron-rich compounds are commonly used as hole-transport materials, since facile hole injection at the anode/HTL interface is believed to promote device function.[7,8] However, hole-transporting materials with a lower redox potential and a lower energetic barrier for hole injection at the anode/HTL interface also have a higher barrier for hole injection into the EL (Figure 2a).

Another pathway for exciton formation is the generation of the EM^{*s} emissive state (EM = electroluminescent moiety) through reaction of the radical cation of the hole-transport material with the $EM^{-\bullet}$ species[9] (Figure 1, reaction 3). This process can occur if the energy difference between the LUMO of the emitter and the HOMO of the hole-transport material is larger than the energy of the EM^{*s} emissive state. This reaction proceeds more readily for larger LUMO(EM)/HOMO(HTM) differences. Figure 2b illustrates how a lower energetic barrier for hole injection at the anode/HTL interface is associated with a smaller driving force for the EM^{*s} formation via this pathway.

Thus, facile hole injection from the anode appears to be counterbalanced by increased energetic barriers for the reactions at the HTL/EL interface. Therefore, it is

[†] California Institute of Technology.
[‡] Optical Sciences Center, University of Arizona.
[§] Department of Chemistry, University of Arizona.

(1) Bässler, H. *Phys. Status Solidi (b)* **1993**, *175*, 15 and references therein.
(2) Van der Auweraer, M.; De Schryver, F. C.; Borsenberger, P. M.; Fitzgerald, J. J. *J. Phys. Chem.* **1993**, *97*, 8808.
(3) Borsenberger, P. M.; Pautmeier, L.; Richert, R.; Bässler, H. *J. Chem. Phys.* **1991**, *94*, 8276.
(4) Gruenbaum, W. T.; Sorriero, L. J.; Borsenberger, P. M.; Zumbulyadis, N. *Jpn. J. Appl. Phys.* **1996**, *35*, 2714.
(5) Heun, S.; Borsenberger, P. M. *Physica B* **1995**, *216*, 43.
(6) Bellmann, E.; Shaheen, S. E.; Thayumanavan, S.; Barlow, S.; Grubbs, R. H.; Marder, S. R.; Kippelen, B.; Peyghambarian, N. *Chem. Mater.* **1998**, *10*, 1668.
(7) Tsutsui, T. *MRS Bull.* **1997**, *June*, 39 and references therein.
(8) Adachi, C.; Nagai, K.; Tamoto, M. *Appl. Phys. Lett.* **1995**, *66*, 2679.
(9) Anderson, J. D.; McDonald, E. M.; Lee, P. A.; Anderson, M. L.; Ritchie, E. L.; Hall, H. K.; Hopkins, T.; Padias, A.; Thayumanavan, S.; Barlow, S.; Marder, S. R.; Jabbour, G. E.; Shaheen, S. E.; Kippelen, B.; Peyghambarian, N.; Wightman, R. M.; Armstrong, N. R. *J. Am. Chem. Soc.* **1998**, *120*, 9646.

10.1021/cm980614r CCC: $18.00
Published on Web 01/21/1999

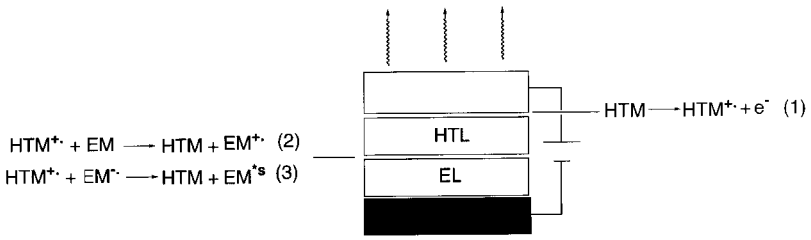

Figure 1. Schematic representation of a two-layer organic LED (HTL = hole-transport layer, EL = electroluminescent layer, HTM = hole-transport moiety, EM = electroluminescent moiety).

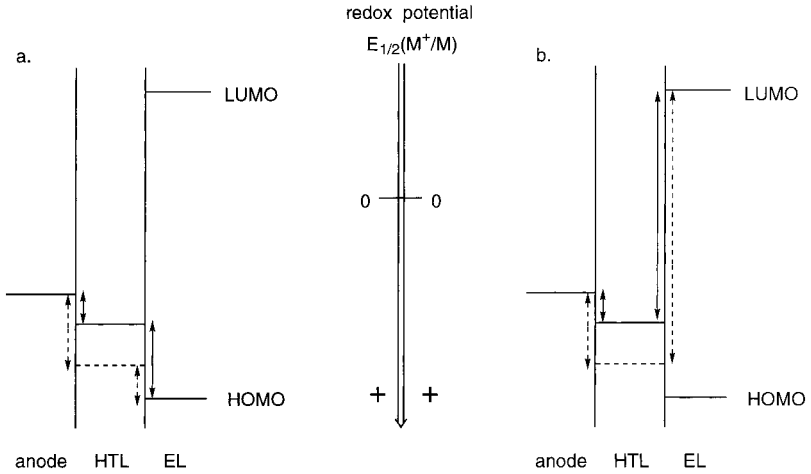

Figure 2. Schematic representation of the energy barriers at the anode/HTL and the HTL/EL interfaces for different redox potentials of the hole-transport material.

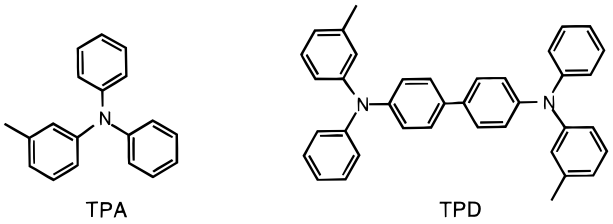

Figure 3. Structures of TPA and TPD.

difficult to predict which redox behavior of the hole-transport material is optimal for the overall device performance. This motivated us to prepare hole-transport polymers with different redox potentials and to examine the effect of the redox potential on the characteristics of a two-layer LED.

We report the synthesis of a series of analogous hole-transport polymers with systematic variation of the redox potential. The hole-transporting functionalities are derivatives of the well-studied organic hole-transporting molecules TPA and TPD[7] (Figure 3). Since high glass transition temperatures have been found to increase the thermal and long-term stability of the device,[10] we have covalently incorporated the TPA and TPD derivatives into high-T_g polymers. Furthermore, by preparing a high molecular weight hole-transporting material, we have achieved desirable film-formation properties. We report device data for two-layer LEDs with ITO as the anode, tris(8-quinolinato)aluminum (Alq) as the electroluminescent material, and magnesium as the cathode.

(10) (a) Tanaka, H.; Tokito, S.; Taga, Y.; Okada, A. *J. Chem. Soc., Chem. Commun.* **1996**, 2175. (b) Thelakkat, M.; Schmidt, H.-W. *Adv. Mater.* **1998**, *10*, 219. (c) Katsuma, K.; Shirota, Y. *Adv. Mater.* **1998**, *10*, 223.

Experimental Section

General. All syntheses were carried out under argon, which was purified by passage through columns of BASF R-11 catalyst (Chemalog) and 4 Å molecular sieves (Linde). NMR spectra were recorded on a GE QE-300 Plus (300 MHz for ^{1}H, 75 MHz for ^{13}C) spectrometer. Gel permeation chromatograms were obtained on a HPLC system using an Altex model 110A pump, a Rheodyne model 7125 injector with a 100 μL injection loop, American Polymer Standards 10 μm mixed bed columns, a Knauer differential refractometer, and CH_2Cl_2 as eluent at a 1.0 mL/min flow rate. Cyclic voltammetry was conducted using a glassy carbon working electrode, a platinum auxiliary electrode, and a AgCl/Ag pseudoreference electrode in 0.1 M solutions of tetrabutylammonium hexafluorophosphate in methylene chloride. Redox potentials were referenced to the ferrocene/ferrocenium couple ($E_{1/2}$ (ferrocenium/ferrocene) = 0 V). Differential scanning calorimetry was carried out on a Perkin-Elmer DSC-7 with a scan rate of 10 °C/min. Thermal gravimetric analysis was performed under nitrogen at a heating rate of 10 °C/min using a Shimadzu TGA-50 device and aluminum pans. UV−vis spectra were recorded using a Hewlett-Packard HP 8453 spectrometer. High-resolution mass spectra were provided by the Southern California Mass Spectrometry Facility (University of California at Riverside) and by Mass Spectrometry Facility of University of California at Los Angeles. Elemental analyses were performed by Midwest Microlabs.

Materials. Toluene and tetrahydrofuran were distilled from Na/benzophenone. Methylene chloride used in cyclic voltammetry measurements was dried and degassed by passage through drying columns.[11] Samples of molecular TPD derivatives were provided by Dr. Stephen Barlow and Dr. S. Thayumanavan. 1-bromo-4-(*m*-tolylphenylamino)benzene (**4b**) was prepared as previously reported.[6] All other reagents and starting materials were purchased from Aldrich Chemical Co. or Strem Chemicals and used as received, unless otherwise noted.

(11) Pangborn, A. B.; Giardello, M. A.; Grubbs, R. H.; Rosen, R. K.; Timmers, F. J. *Organometallics* **1996**, *15*, 1518.

Preparation of 4-Bromo-4′-(*m*-tolyl-*p*-methoxyphenylamino)biphenyl (1a). Tris(dibenzylideneacetone)dipalladium(0) (Pd_2dba_3) (618 mg, 0.67 mmol), 1,1′-bis(diphenylphosphino)ferrocene (dppf) (561 mg, 1 mmol), and 3-bromotoluene (7.7 g, 45 mmol) were dissolved in 400 mL of dry toluene and stirred for 15 min. Sodium *tert*-butoxide (5.2 g, 54 mmol) and *p*-methoxyaniline (5.5 g, 45 mmol) were then added. The reaction mixture was warmed to 100 °C for 3 h. Thereafter, 4,4′-dibromobiphenyl (42 g, 135 mmol) and sodium *tert*-butoxide (5.2 g, 54 mmol) were added, and the reaction mixture was heated to 100 °C for 16 h. The reaction mixture was partitioned between water and ether, and the aqueous layer was extracted with ether. The combined organic fractions were dried over $MgSO_4$, and the solvent was evaporated under reduced pressure. Column chromatography (silica, hexanes) afforded 19.3 g (84%) of product **1a**: ^{1}H NMR (CD_2Cl_2) δ 7.57−7.37 (m, 6H), 7.15−6.97 (m, 6H), 6.91−6.80 (m, 4H), 3.78 (s, 3H), 2.24 (s, 3H); ^{13}C NMR (CD_2Cl_2) δ 157.1, 148.7, 148.3, 141.0, 140.2, 139.7, 132.8, 132.4, 129.6, 128.6, 128.1, 127.9, 124.9, 124.1, 122.7, 121.4, 121.1, 115.4, 56.0, 21.8; HRMS calcd for $C_{26}H_{22}{}^{81}$BrNO [M^+] 445.0885, found 445.0864. Anal. Calcd for $C_{26}H_{22}$BrNO: C, 69.94; H, 4.46; N, 3.26. Found: C, 69.69; H, 4.49; N, 3.15.

Preparation of 4-Bromo-4′-(*m*-tolylphenylamino)biphenyl (2a). 2a was prepared by analogy to **1a** using aniline instead of *p*-methoxyaniline in 66% yield: ^{1}H NMR (CD_2Cl_2) δ 7.58−7.53 (m, 2H), 7.49−7.43 (m, 4H), 7.29 (dt, J = 2.1, 7.8 Hz, 2H), 7.19 (bd t, J = 7.8 Hz, 1H), 7.14−7.03 (m, 5H), 6.98 (bd s, 1H), 6.92 (bd dt, 2H, J = 1.8, 7.6 Hz, 2H), 2.24 (s, 3H); ^{13}C NMR (CD_2Cl_2) δ 147.5, 147.4, 147.2, 139.3, 139.1, 133.0, 131.5, 129.0, 128.9, 127.9, 127.2, 125.1, 124.1, 123.9, 123.2, 122.7, 121.6, 120.5, 20.9; HRMS calcd for $C_{25}H_{20}{}^{81}$BrN [M^+] 415.0759, found 415.0753. Anal. Calcd for $C_{25}H_{20}$BrN: C, 72.47; H, 4.87; N, 3.38. Found: C, 72.24; H, 4.82; N, 3.34.

Preparation of 4-Bromo-4′-(*m*-tolyl-*m*-fluorophenylamino)biphenyl (3a). 3a was prepared by analogy to **1a** using *m*-fluoroaniline instead of *p*-methoxyaniline in 62% yield: ^{1}H NMR (CD_2Cl_2) δ 7.60−7.42 (m, 6H), 7.25−7.12 (m, 4H), 7.02−6.67 (m, 6H), 2.24 (s, 3H); ^{13}C NMR (CD_2Cl_2) δ 165.7, 162.4, 150.2, 150.0, 147.6, 147.4, 140.2, 140.0, 134.9, 132.4, 130.9, 130.7, 129.9, 128.8, 128.3, 126.7, 125.6, 125.1, 123.2, 121.6, 119.1, 110.5, 110.2, 109.5, 109.2, 21.8; HRMS calcd for $C_{25}H_{19}{}^{79}BrF_2N$ [M^+] 433.0664, found 433.0663. Anal. Calcd for $C_{25}H_{19}BrFN$: C, 69.45; H, 4.43; N, 3.24. Found: C, 69.66; H, 4.45; N, 3.28.

Preparation of 4-Bromo-4′-(*m*-tolyl-3,5-difluorophenylamino)biphenyl (5a). 5a was prepared by analogy to **1a** using 3,5-difluoroaniline instead of *p*-methoxyaniline in 69% yield: ^{1}H NMR (CD_2Cl_2) δ 7.60−7.42 (m, 8H), 7.25−7.15 (m, 4H), 7.01 (bd m, 2H), 6.53 (m, 2H), 6.38 (m, 1H), 2.24 (s, 3H); ^{13}C NMR (CD_2Cl_2) δ 165.9, 165,7 162.6, 162.4, 150.9, 146.8, 146.7, 140.4, 139.9, 136.0, 132.4, 130.0, 128.9, 128.4, 127.3, 126.4, 126.0, 123.8, 121.9, 121.7, 104.7, 104.6, 104.5, 104.3, 97.2, 96.8, 96.5, 21.8; HRMS calcd for $C_{25}H_{18}{}^{79}BrF_2N$ [M^+] 449.0583, found 449.0590. Anal. Calcd for $C_{25}H_{18}BrF_2N$: C, 66.68; H, 4.03; N, 3.11. Found: C, 66.36; H, 4.00; N, 3.11.

Preparation of 4-(*m*-Tolyl-*p*-methoxyphenylamino)-4′-(*p*-methoxybenzyl-*p*-bromophenylamino)biphenyl (1b). 1b was prepared by analogy to **1a** from **1a** and *p*-methoxyaniline followed by the addition of 1,4-dibromobenzene in 65% yield. Purification was accomplished by column chromatography on silica gel with hexanes followed by 20% toluene in hexanes: ^{1}H NMR (CD_2Cl_2) δ 7.41 (bd t, J = 8.1 Hz, 4H), 7.29 (bd d, J = 8.7 Hz, 2H), 7.06 (m, 10H), 6.87 (m, 8H), 3.78 (s, 6H), 2.24 (s, 3H); ^{13}C NMR (CD_2Cl_2) δ 157.3, 156.9, 148.5, 147.9, 146.9, 141.1, 140.5, 139.6, 135.3, 134.0, 132.5, 129.5, 128.1, 127.9, 127.7, 127.6, 124.5, 124.3, 124.0, 123.7, 123.1, 121.0, 115.4, 115.3, 114.1, 56.0, 21.8; HRMS calcd for $C_{39}H_{33}{}^{81}BrN_2O_2$ [M^+] 642.1705, found 642.1711. Anal. Calcd for $C_{39}H_{33}BrN_2O_2$: C, 73.01; H, 5.18; N, 4.37. Found: C, 72.82; H, 5.15; N, 4.31.

Preparation of 4-(*m*-Tolylphenylamino)-4′-(*m*-tolyl-*p*-bromophenylamino)biphenyl (2b). 2b was prepared by analogy to **1a** from **2a** and 3-aminotoluene followed by the addition of 1,4-dibromobenzene in 63% yield. Purification was accomplished by column chromatography on silica gel with hexanes followed by 20% toluene in hexanes: ^{1}H NMR (CD_2Cl_2) δ 7.50−7.40 (m, 4H), 7.35−7.30 (m, 2H), 7.28−7.21 (m, 2H), 7.18−7.00 (m, 9H), 6.98−6.85 (m, 8H), 2.24 (s, 6H); ^{13}C NMR (CD_2Cl_2) δ 148.3, 148.1, 147.7, 147.6, 147.5, 146.9, 140.0, 139.8, 135.7, 134.8, 132.6, 129.7, 129.6, 129.5, 128.7, 127.8, 127.7, 126.0, 125.7, 125.6, 124.94, 124.87, 124.76, 124.5, 124.4, 123.3, 122.4, 122.2, 115.0, 21.8; HRMS calcd for $C_{38}H_{31}{}^{81}BrN_2$ [M^+] 596.1650, found 596.1649. Anal. Calcd for $C_{38}H_{31}BrN_2$: C, 76.63; H, 5.25; N, 4.70. Found: C, 76.85; H, 5.55; N, 4.36.

Preparation of 4-(*m*-Tolyl-*m*-fluorophenylamino)-4′-(*m*-fluorophenyl-*p*-bromophenylamino)biphenyl (3b). 3b was prepared by analogy to **1a** from **3a** and *m*-fluoroaniline followed by the addition of 1,4-dibromobenzene in 63% yield. Purification was accomplished by column chromatography on silica gel with hexanes followed by 10% ethyl acetate in hexanes: ^{1}H NMR (CD_2Cl_2) δ 7.52 (dd, J = 8.4, 6.3 Hz, 4H), 7.41 (d, J = 8.7 Hz, 2H), 7.28−7.12 (m, 8H), 7.07−6.93 (m, 5H), 6.90−6.65 (m, 5H), 2.24 (s, 3H); ^{13}C NMR (CD_2Cl_2) δ 164.8, 161.6, 149.4, 149.3, 148.8, 148.6, 146.6, 146.2, 146.0, 145.5, 139.3, 135.7, 134.7, 132.1, 130.1, 130.0, 129.9, 129.8, 129.0, 128.7, 127.9, 127.8, 127.2, 125.8, 125.6, 124.8, 124.5, 124.4, 122.2, 118.5, 118.0, 115.5, 110.0, 109.6, 109.4, 109.1, 109.0, 108.8, 108.3, 108.0, 21.8; HRMS calcd for $C_{37}H_{27}{}^{81}BrF_2N_2$ [M^+] 618.1305, found 618.1310. Anal. Calcd for $C_{37}H_{27}BrF_2N_2$: C, 71.97; H, 4.41; N, 4.54. Found: C, 72.13; H, 4.81; N, 4.73.

Preparation of 4-(*m*-Tolyl-3,5-difluorophenylamino)-4′-(3,5-difluorophenyl-*p*-bromophenylamino)biphenyl (5b). 5b was prepared by analogy to **1a** from **5a** and 3,5-difluoroaniline followed by the addition of 1,4-dibromobenzene in 62% yield. Purification was accomplished by column chromatography on silica gel with hexanes followed by 20% toluene in hexanes: ^{1}H NMR (CD_2Cl_2) δ 7.67−7.62 (m, 2H), 7.58−7.49 (m, 4H), 7.34−7.11 (m, 8H), 7.02−6.93 (m, 3H), 6.86−6.80 (m, 1H), 6.53−6.31 (m, 4H), 2.24 (s, 3H); ^{13}C NMR (CD_2Cl_2) δ 165.5, 165.3, 165.0, 164.9, 164.8, 150.8, 150.65, 150.5, 146.4, 145.8, 145.7, 140.3, 140.0, 136.4, 135.5, 132.7, 132.6, 130.4, 129.7, 129.2, 128.4, 128.0, 127.9, 127.8, 126.9, 125.9, 125.4, 123.4, 122.8, 121.3, 104.2, 104.1, 103.9, 103.8, 103.7, 98.0, 97.6, 96.6, 96.2, 95.9, 95.5, 95.1, 94.8, 21.8; HRMS calcd for $C_{37}H_{25}{}^{79}BrF_4N_2$ [M^+] 652.1135, found 652.1137. Anal. Calcd for $C_{37}H_{21}BrN_2F_4$: C, 68.04; H, 3.24; N, 4.28. Found: C, 68.17; H, 3.44; N, 4.11.

Preparation of 4-(*m*-Tolyl-*p*-methoxyphenylamino)-4′-(*p*-methoxyphenyl-*p*-vinylphenylamino)biphenyl (1). *Method 1.* **1b** (3 g, 4.67 mmol), palladium acetate (26.2 mg, 0.12 mmol), and tris(*o*-tolyl)phosphine were dissolved in 15 mL of toluene. Diethoxymethylvinylsilane (2.25 g, 14 mmol) and tributylammoniumfluoride (21 mL of a 1M solution in tetrahydrofuran, 14 mmol) were added to the solution, and the reaction mixture was heated to 100 °C for 4 h.

Method 2. **1b** (3 g, 4.67 mmol), tetrakis(triphenylphosphine)-palladium(0) (136 mg, 0.12 mmol), and 2,6-di-*tert*-butyl-4-methylphenol (2−5 mg) were dissolved in 25 mL of toluene. Tributyl(vinyl)tin (1.8 g, 5.6 mmol) was added to the solution, and the mixture was heated to 100 °C for 3 h. Purification of the product was achieved through column chromatography (silica, 10% ethyl acetate in hexanes).

The yields were 83% for method 1 and 92% for method 2: ^{1}H NMR (CD_2Cl_2) δ 7.46−7.38 (m, 4H), 7.30−7.20 (m, 2H), 7.16−6.97 (m, 12H), 6.94−6.89 (m, 6H), 6.66 (dd, J = 10.8, 17.7 Hz, 1H), 5.63 (d, J = 17.7 Hz, 1H), 5.13 (d, J = 10.8 Hz, 1H), 3.78 (s, 6H), 2.24 (s, 3H); ^{13}C NMR (CD_2Cl_2) δ 157.1, 156.9, 148.5, 148.3, 147.8, 147.6, 143.3, 141.1, 140.8, 139.6, 136.8, 134.9, 134.5, 134.2, 134.1, 131.7, 129.7, 129.5, 128.0, 127.9, 127.5, 124.5, 123.8, 123.6, 123.5, 123.4, 123.2, 122.8, 122.7, 122.5, 121.0, 115.4, 115.3, 112.1, 56.0, 21.8; HRMS calcd for $C_{41}H_{36}N_2O_2$ [M^+] 588.2777, found 588.2787. Anal. Calcd for $C_{41}H_{36}N_2O_2$: C, 83.64; H, 6.16; N, 4.76. Found: C, 83.74; H, 6.52; N, 4.63.

Preparation of 4-(*m*-Tolylphenylamino)-4′-(*m*-tolyl-*p*-vinylphenylamino)biphenyl (2). 2 was prepared by

analogy to **1** from **2b** in yields of 64% for method 1 and 76% for method 2. Purification was accomplished by column chromatography on silica gel with 5% ethyl acetate in hexanes: ^{1}H NMR (CD_2Cl_2) δ 7.45 (dd, J = 2.4, 8.7 Hz, 4H), 7.32−7.22 (m, 4H), 7.18−6.97 (m, 12H), 6.95−6.85 (m, 5H), 6.66 (dd, J = 11.1, 17.7 Hz, 1H), 5.64 (d, J = 17.7 Hz, 1H), 5.13 (d, J = 11.1 Hz, 1H), 2.24 (s, 6H); ^{13}C NMR (CD_2Cl_2) δ 148.3, 148.1, 148.0, 147.9, 147.4, 147.1, 139.9, 139.8, 136.7, 135.3, 135.0, 134.9, 133.5, 132.3, 129.7, 129.6, 129.2, 127.7, 127.5, 125.9, 125.7, 124.8, 124.4, 124.0, 123.2, 122.4, 122.2, 112.4, 21.8; HRMS calcd for $C_{40}H_{34}N_2$ [M^+] 542.2722, found 542.2728. Anal. Calcd for $C_{40}H_{34}N_2$: C, 88.52; H, 6.31; N, 5.16. Found: C, 88.53; H, 6.58; N, 4.98.

Preparation of 4-(*m*-Tolyl-*m*-fluorophenylamino)-4′-(*m*-fluorophenyl-*p*-vinylphenylamino)biphenyl (3). 3 was prepared by analogy to **1** from **3b** in yields of 66% for method 1 and 92% for method 2. Purification was accomplished by column chromatography on silica gel with 20% toluene in hexanes: ^{1}H NMR (CD_2Cl_2) δ 7.53−7.45 (m, 4H), 7.36−7.26 (m, 2H), 7.22−7.04 (m, 9H), 6.93 (bd t, J = 7.8 Hz, 3H), 6.87−6.62 (m, 7H), 5.67 (d, J = 17.7 Hz, 1H), 5.18 (d, J = 11.1 Hz, 1H), 2.24 (s, 6H); ^{13}C NMR (CD_2Cl_2) δ 165.6, 162.4, 150.3, 150.1, 149.9, 149.8, 147.5, 147.2, 147.0, 146.6, 140.1, 136.6, 136.2, 136.0, 135.7, 130.6, 130.0, 129.8, 128.3, 128.0, 127.7, 126.5, 125.6, 125.4, 125.3, 125.1, 124.3, 123.0, 119.2, 118.8, 113.1, 110.6, 110.3, 110.2, 110.0, 109.9, 109.6, 109.3, 109.1, 109.0, 108.8, 21.8; HRMS calcd for $C_{39}H_{30}N_2F_2$ [M^+] 564.2377, found 564.2397. Anal. Calcd for $C_{39}H_{30}N_2F_2$: C, 82.96; H, 5.35; N, 4.96. Found: C, 82.78; H, 5.43; N, 4.85.

Preparation of *m*-Tolyl(*p*-vinylphenyl)phenylamine (4). 4 was prepared by analogy to **1** from **4b** in yields of 66% for method 1 and 89% for method 2. Purification was accomplished by column chromatography on silica gel with hexanes: ^{1}H NMR (CD_2Cl_2) δ 7.35−7.25 (m, 4H), 7.18 (bd t, J = 7.8 Hz, 1H), 7.13−7.01 (m, 5H), 7.18−6.88 (m, 3H), 6.70 (dd, J = 10.8, 17.7 Hz, 1H), 5.67 (d, J = 17.7 Hz, 1H), 5.13 (d, J = 10.8 Hz, 1H), 2.24 (s, 6H); ^{13}C NMR (CD_2Cl_2) δ 147.75, 147.70, 147.6, 139.3, 136.3, 131.7, 129.3, 129.1, 127.0, 125.3, 124.3, 124.1, 123.4, 122.9, 121.8, 111.9, 21.8; HRMS calcd for $C_{21}H_{19}N$ [M^+] 285.1512, found 285.1517. Anal. Calcd for $C_{21}H_{19}N$: C, 88.38; H, 6.71; N, 4.91. Found: C, 88.08; H, 6.85; N, 4.69.

Preparation of 4-(*m*-Tolyl-3,5-difluorophenylamino)-4′-(3,5-difluorophenyl-*p*-vinylphenylamino)biphenyl (5). 5 was prepared by analogy to **1** from **5b** using method 2 in 78% yield. Purification was accomplished by column chromatography on silica gel with 20% toluene in hexanes: ^{1}H NMR (CD_2Cl_2) δ 7.62−7.51 (m, 6H), 7.43−7.37 (m, 2H), 7−29−7.13 (m, 6H), 7.05−6.96 (m, 3H), 6.92−6.75 (m, 2H), 6.57−6.34 (m, 4H), 5.86 (d, J = 17.7 Hz, 1H), 5.34 (d, J = 10.8 Hz, 1H), 2.24 (s, 6H); ^{13}C NMR (CD_2Cl_2) δ 165.9, 165.7, 165.2, 165.0, 163.1, 162.8, 162.7, 162.5, 161.9, 161.7, 159.8, 159.6, 151.2, 151.0, 150.9, 146.8, 146.1, 144.8, 144.7, 144.6, 141.0, 140.4, 138.3, 136.8, 135.7, 131.4, 131.1, 130.0, 129.5, 128.7, 128.2, 128.1, 127.5, 127.3, 126.3, 125.8, 123.7, 121.6, 115.2, 104.4, 104.1, 98.2, 97.9, 96.9, 96.6, 96.2, 95.7, 95.4, 95.0, 21.8; HRMS calcd for $C_{39}H_{28}N_2F_4$ [M^+] 600.2174, found 600.2188. Anal. Calcd for $C_{39}H_{24}N_2F_4$: C, 77.99; H, 4.03; N, 4.68. Found: C, 77.89; H, 4.17; N, 4.52.

General Polymerization Procedure. The monomer (1.5 mmol, 500 mg to 1 g) was dissolved in a solvent mixture of 2 mL of toluene and 0.2 mL of THF. The solution was cooled to −78 °C and the polymerization was initiated through injection of *n*-butyllithium (0.075 mmol, 46.9 μL of a 1.6 M solution in hexanes). The polymerization was allowed to proceed for 1 h at −78 °C. The reaction mixture was poured into methanol to precipitate the polymer. The polymers were purified by redissolving in methylene chloride and repricipitation into methanol several times and drying in vacuo. **P1, P2, P3,** and **P4** were prepared using this procedure. In the case of **P5**, the monomer was dissolved in 5 mL of THF and 3.075 mmol of *n*-butyllithium was added to initiate. During the purification of **P5**, an insoluble fraction was removed by filtration.

P1: 96% yield; ^{1}H NMR (CD_2Cl_2) δ 7.4 (bd), 7.1 (bd), 6.8 (bd), 6.5 (bd), 3.7 (bd), 3.4 (bd), 2.2 (bd, two overlapping signals), 1.6 (bd).

P2: 98% yield; ^{1}H NMR (CD_2Cl_2) δ 7.4 (bd), 7.1 (bd), 6.8 (bd), 2.3 (bd), 2.2 (bd), 1.6 (bd).

P3: 98% yield; ^{1}H NMR (CD_2Cl_2) δ 7.5 (bd), 7.2 (bd), 6.9 (bd), 6.5 (bd), 2.3 (bd), 2.2 (bd), 1.6 (bd).

P4: 96% yield; ^{1}H NMR (CD_2Cl_2) δ 7.2−6.5 (bd), 2.2 (bd, two overlapping signals), 1.6 (bd).

P5: 65% yield; ^{1}H NMR (CD_2Cl_2) δ 7.4 (bd), 7.0 (bd), 6.9 (bd), 6.4 (bd), 6.3 (bd), 2.2 (bd, two overlapping signals), 1.6 (bd).

Fabrication and Characterization of Light-Emitting Devices. Devices were fabricated on ITO-coated glass substrates (Donnelly Corp.) with a nominal sheet resistance of 20 Ω/sq which had been ultrasonicated in acetone, methanol, and 2-propanol, dried in a stream of nitrogen, and then plasma etched for 60 s. Polymer layers (40 nm) were formed by spin casting from chlorobenzene solutions (10 g/L). The second layer consisted of vacuum vapor deposited Alq (60 nm), which had been purified by recrystallization and sublimation prior to deposition. Mg cathodes (200 nm) were thermally deposited at a rate of 8 Å/s through a shadow mask to create devices 3 × 5 mm^2 in area. Current−voltage and light output characteristics of the devices were measured in forward bias. Device emission was measured using a silicon photodetector at a fixed distance from the sample (12 cm). The response of the detector had been calibrated using several test devices, for which the total power emitted in the forward direction was measured with a NIST traceable integrating sphere (Labsphere). Photometric units of cd/m^2 were calculated using the forward output power and the electroluminescence spectra of the devices. Efficiencies were measured in units of external quantum efficiency (percent photons/electron). Cathode deposition and device characterization were performed in a nitrogen drybox (Vacuum Atmospheres).

Results and Discussion

Previous studies have suggested that polymers with nonpolar compact backbones exhibit higher hole mobilities and show improved performance as hole-transport layers in LEDs.[1−6] Therefore, the monomers were designed to contain a styrene type functionality, which would permit anionic polymerization, yielding an all-hydrocarbon compact backbone (Figure 4). Electron-donating and electron-withdrawing substituents have been introduced on TPD to vary the redox potential of the hole-transporting moiety.

Monomer Synthesis. We have prepared different monovinylated TPD derivatives by an efficient three-step procedure based on palladium-catalyzed amination[12−15] (Scheme 1). This methodology allows for independent selection of the substituent patterns of the four outer phenyl rings. The TPA monomer **4** was synthesized in a fashion similar to the TPD derivatives (Scheme 1).

In the last step of the monomer synthesis, the monovinyl compounds **1**−**5** were obtained by palladium-catalyzed vinylation. The desired products were prepared in high yield using the tin reagent **6**[16] or an excess of the silicon reagent **7**[17] (Scheme 1). Nickel-catalyzed

(12) Wolfe, J. P.; Rennels, R. A.; Buchwald, S. L. *Tetrahedron* **1996**, *52*, 7525.
(13) Wolfe, J. P.; Wagaw, S.; Buchwald, S. L. *J. Am. Chem. Soc.* **1996**, *118*, 7215.
(14) Driver, M. S.; Hartwig, J. F. *J. Am. Chem. Soc.* **1996**, *118*, 7217.
(15) Thayumanavan, S.; Barlow, S.; Marder, S. R. *Chem. Mater.* **1997**, *9*, 3231.
(16) McKean, D. R.; Parrinello, G.; Renaldo, A. F.; Stille, *J. Org. Chem.* **1987**, *52*, 422.
(17) Hatanaka, Y.; Hiyama, T. *J. Org. Chem.* **1989**, *54*, 268.

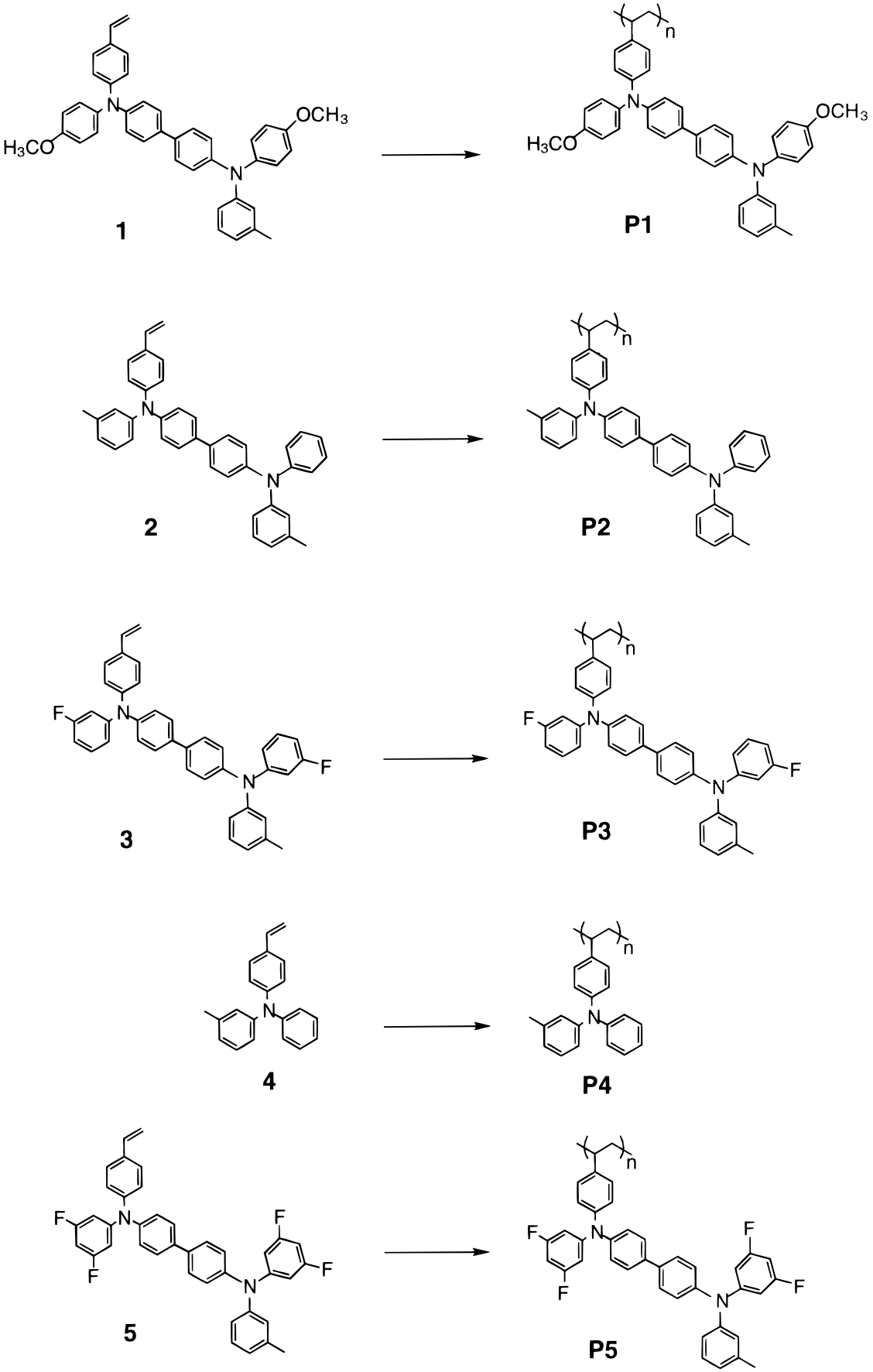

Figure 4. Structures of the synthesized hole-transporting polymers and the corresponding monomers.

reaction of the bromo derivatives **1b**−**5b** with vinyl-Grignard[18,19] did not result in formation of the desired product. Another synthetic route toward **1**−**5** involves substitution of the bromine in **1b**−**5b** by an aldehyde

Scheme 1

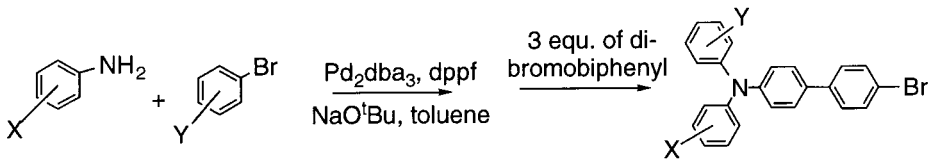

60 - 70 %

1a: Ar-X = *p*-methoxyphenyl, Ar-Y = *m*-tolyl
2a: Ar-X = *m*-tolyl, Ar-Y = phenyl
3a: Ar-X = *m*-fluorophenyl, Ar-Y = *m*-tolyl
5a: Ar-X = 3,5-difluorophenyl, Ar-Y = *m*-tolyl

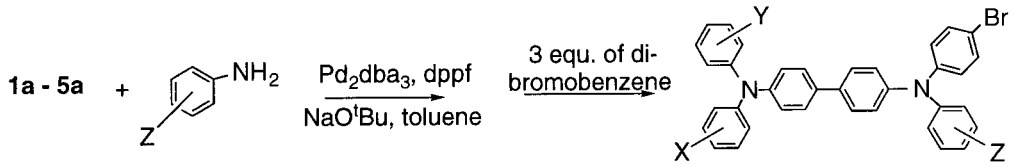

60 -70 %

1b: Ar-X, Ar-Z = *p*-methoxyphenyl, Ar-Y = *m*-tolyl
2b: Ar-X, Ar-Z = *m*-tolyl, Ar-Y = phenyl
3b: Ar-X, Ar-Z = *m*-fluorophenyl, Ar-Y = *m*-tolyl
5b: Ar-X, Ar-Z = 3,5-difluorophenyl, Ar-Y = *m*-tolyl

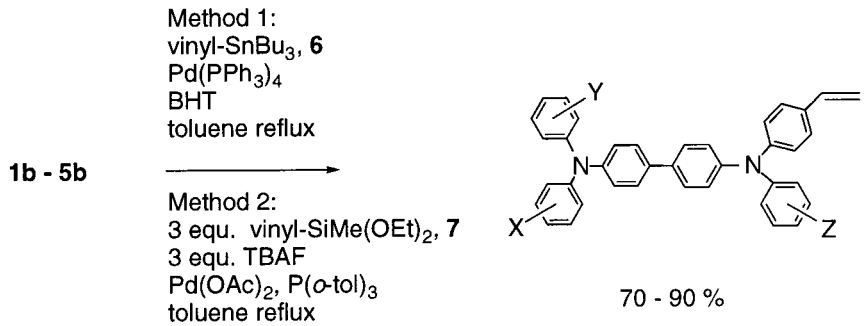

70 - 90 %

1: Ar-X, Ar-Z = *p*-methoxyphenyl, Ar-Y = *m*-tolyl
2: Ar-X, Ar-Z = *m*-tolyl, Ar-Y = phenyl
3: Ar-X, Ar-Z = *m*-fluorophenyl, Ar-Y = *m*-tolyl
5: Ar-X, Ar-Z = 3,5-difluorophenyl, Ar-Y = *m*-tolyl

Pd_2dba_3 = Tris(dibenzylideneacetone)dipalladium(0), dppf = Bis(diphenylphosphino)ferrocene, BHT = 2,6-Di-*tert*-butyl-4-methylphenol, TBAF = Tributylammoniumfluoride

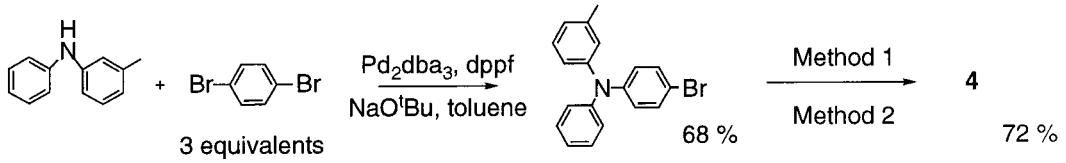

4b

group via lithiation and quenching with dimethylformamide, followed by reaction of the aldehyde with the appropriate Wittig reagent or titanium reagent[20] to form the vinyl group. The transformation of **1b**−**5b** to **1**−**5** via the aldehyde, however, afforded considerably lower yields (approximately 40%) of the monovinyl product.

Table 1. Polymer Properties

polymer	yield[a] (%)	M_W[b]	PDI[b]	T_g (°C)	T_{TGA}[c] (°C)	λ_{max}[d] (nm)
P1	96	15 700	1.28	132	408	360, 312
P2	98	11 150	1.13	151	400	358, 312
P3	98	15 100	1.16	147	414	353, 312
P4	96	5 000	1.09	104	397	307
P5	65	6 550	1.30	140	412	338, 315

[a] Isolated yield. [b] Determined by gel permeation chromatography in methylene chloride versus monodispersed polystyrene standards. [c] Temperature of thermal decomposition determined by thermal gravimetric analysis and reported as temperature of onset of weight loss. [d] Absorption spectrum in methylene chloride solution.

Table 2. Redox Potentials of the HTL Polymers[a]

	polymers		model small molecules	
polymers	$^1E_{1/2}$[b] (mV)	$^2E_{1/2}$[c] (mV)	$^1E_{1/2}$[b] (mV)	$^2E_{1/2}$[c] (mV)
P1	150	355	160	400
P2	280	480	260	510
P3	390	560	360	580
P4	$E_{ox} = 490$, $E_{red} = 380$[d]		$E_{ox} = 550$, $E_{red} = 470$[d]	
P5	490	590	510	660

[a] Error of the measurement is estimated to ±10 mV. [b] $^1E_{1/2} = E_{1/2}(M^+/M)$. [c] $^2E_{1/2} = E_{1/2}(M^{2+}/M^+)$. [d] Irreversible redox potential.

Polymerization. The anionic polymerization of monomers **1**−**4** was initiated by 0.05 equiv of *n*-butyllithium (*n*-BuLi) at −78 °C. In the case of monomer **5**, the two fluorine substituents in the 3- and 5-position of the outer phenyl rings cause the para-hydrogens to be reactive toward strong bases. *n*-BuLi was observed to deprotonate the TPD core prior to initiating polymerization by a deuterium quenching experiment. The polymerization of the dianion was possible in a dilute THF solution and yielded the target polymer after quenching with methanol at −78 °C. The isolated yield of polymer **P5** is lower than the yields of polymers **P1**−**P4**, because an insoluble fraction had to be removed by filtration. This insoluble material is presumably produced by crosslinking during the polymerization.

All of the resulting polymers exhibit high glass transition temperatures (T_g), high thermal stability (up to 400 °C by themal gravimetric analysis), and good solubility. The polymers form high-quality transparent thin films upon spin casting, and the solutions and films fluoresce blue. The polymer properties are summarized in Table 1.

Cyclic Voltammetry. The redox potentials of the polymers have been determined by cyclic voltammetry in methylene chloride versus ferrocenium/ferrocene (Table 2). The cyclic voltammograms for polymers **P1**−**P3** and **P5** show two sequential one-electron processes, corresponding to removal of two electrons from each TPD unit. These redox potentials are similar to the redox potentials of the corresponding molecular compounds,[15] demonstrating that incorporation of TPD into this kind of polymeric framework does not alter its redox behavior. The peak potentials in forward and reverse bias differ by approximately 59 mV, and the peak currents in forward and reverse bias are of similar magnitude. This suggests that the redox potentials are reversible. The cyclic voltammogram for the TPA-based polymer **P4** shows an irreversible redox process at a potential that is lower than the redox potential of the molecular TPA. Simple triarylamines without para-substitution are known to exhibit similar irreversible electrochemistry.[21]

Table 3. Device Characteristics versus Redox Potential of the Hole-Transporting Polymer for the Devices ITO/HTL/Alq/Mg

HTL polymer	$^1E_{1/2}$[a] (mV)	current density at 9 V (mA/cm^2)	max. ext quant efficiency (% photons/e$^-$)	light output at 10 V (cd/m^2)
P1	150	53.4	0.61	2300
P2	280	39.7	1.09	2900
P3	390	28.7	1.25	3700
P4	435[b]	27.4	1.22	1800
P5	490	15.4	1.00	1000

[a] $^1E_{1/2} = E_{1/2}(M^+/M)$; determined by cyclic voltammetry in methylene chloride solution versus ferrocenium/ferrocene. [b] Irreversible redox potential estimated from $(E_{ox} + E_{red})/2$.

The cyclic voltammetry measurements show that polymer **P1** has the lowest barrier for oxidation at the ITO/HTL interface, but its radical cation is hardest to reduce at the HTL/Alq interface. Therefore, **P1** should readily form radical cations at the ITO/HTL interface (Figure 1, reaction 1), but the reaction of these radical cations with Alq (hole injection into EL; Figure 1, reaction 2 and Figure 2a) and with $Alq^{-\bullet}$ radical anions (direct formation of the Alq^{*s} emissive state at the HTL/EL interface;[9] Figure 1, reaction 3 and Figure 2b) should be disfavored. In the case of **P5**, the hole injection at the ITO/HTL interface should be disfavored, but the relevant redox reactions at the HTL/Alq interface should occur more readily. **P2, P3**, and **P4** represent intermediate cases between **P1** and **P5**.

The results of the solution phase cyclic voltammetry measurements herein expose the trends in redox behavior of the polymeric materials relative to each other. Electrochemistry has previously been shown to give qualitative estimates of energy levels in devices.[9] Photoelectron spectroscopic analysis is currently in progress and should give quantitative solid-state energies.

Light-Emitting Diodes. Two-layer LEDs have been prepared using the polymers **P1**−**P5** as hole-transport materials. The devices show typical Alq emission,[22] resulting in green LEDs with a peak emission of 525 nm. Table 3 and Figure 5 summarize the device data.

The maximum external quantum efficiency increases substantially as the redox potential becomes more positive (compare **P1, P2**, and **P3**). Thus, this study suggests that higher external quantum efficiencies can be achieved with hole-transporting materials which are less electron-rich than the commonly used TPD. An optimum value for the HTL redox potential appears to exist around 400 mV versus ferrocenium/ferrocene (**P3**). If the redox potential is increased further than that, the energetic barrier for the reactions 2 and 3 (Figure 1) at the HTL/Alq interface is further decreased but the barrier for hole injection into the HTL (Figure 2)

(18) Tamao, K.; Sumitani, K.; Kumada, M. *J. Am. Chem. Soc.* **1972**, *94*, 4374.
(19) Nugent, W. A.; McKinney, R. J. *J. Org. Chem.* **1985**, *50*, 5370.
(20) Pine, S. H. *Org. React.* **1993**, *43*, 1.
(21) Yano, M.; Furuichi, M.; Sato, K.; Shiomi, D.; Ichimura, A.; Abe, K.; Takui, T.; Itoh, K. *Synth. Met.* **1997**, *85*, 1665.
(22) Tang, C. W.; VanSlyke, S. A. *Appl. Phys. Lett.* **1987**, *51*, 913.

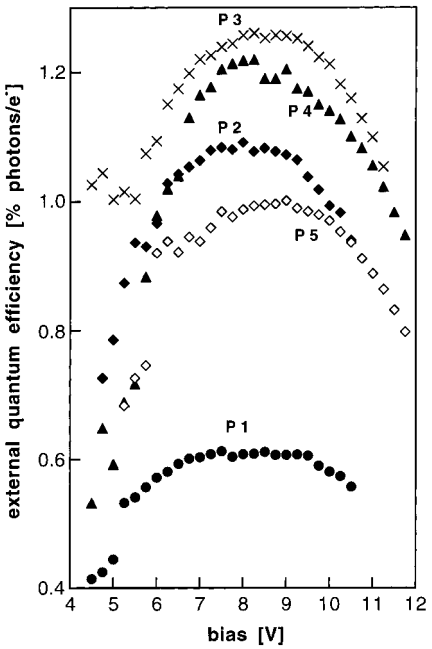

Figure 5. External quantum efficiency versus bias voltage for the devices ITO/HTL/Alq/Mg with polymers **P1**−**P5** as hole-transport materials.

presumably becomes too high. This apparently causes the external quantum efficiency to decrease again (compare **P3, P4**, and **P5**).

Another possible explanation for decreased external quantum efficiencies at too high redox potentials could be the following: electron-withdrawing substituents decrease not only the HOMO energy but also, to a lesser extent, the LUMO energy of a compound.[23] A lower LUMO level of the hole-transport material could result in less efficient electron blocking at the HTL/Alq interface, which would decrease device efficiency.

The current density at 9 V decreases as the redox potential of the HTL increases (Table 3). This is consistent with an increase in the energetic barrier for hole injection from the ITO, and this same trend has been seen in previous work.[24]

To test the stability of the devices, the LEDs were operated at 6 mA constant current (corresponds to 50 mA/m^2) in a nitrogen-filled drybox. Constant current, which is the standard mode for testing OLED lifetimes, drives the same number of charge carriers through the devices with different HTL materials. The observed changes in external quantum efficiency are illustrated in Figure 6. The device with **P1** as hole-transporting material was the least efficient at the beginning of the lifetime study, but in the end the device retained 60% of its initial efficiency after 1 h of continuous operation. Devices which contained **P3**, **P4**, and **P5** decomposed rapidly. After 1 h the trend in performance was reversed with ITO/**P1**/Alq/Mg, showing the highest external quantum efficiency (Figure 6, Table 3). This observation is consistent with a previous study,[8] where it was shown

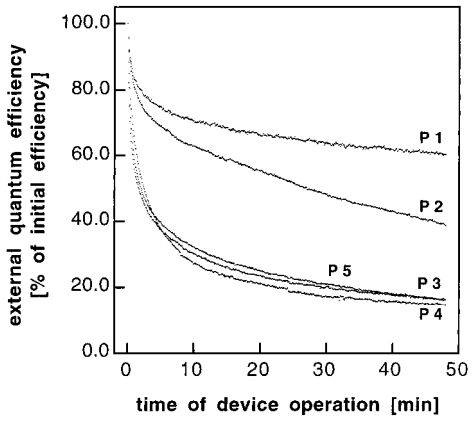

Figure 6. Lifetime study for the devices ITO/HTL/Alq/Mg with polymers **P1**−**P5** as hole-transport materials.

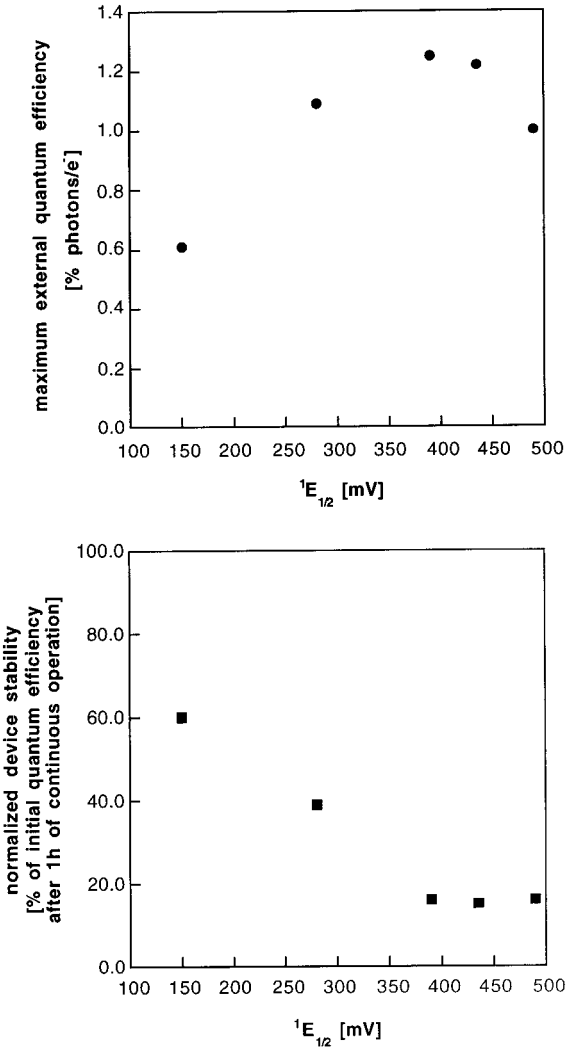

Figure 7. Device characteristics of a two-layer LED ITO/HTL/Alq/Mg versus the redox potential of the hole-transport polymer. ($^1E_{1/2}$ is reported versus ferrocenium/ferrocene.)

that device lifetime is strongly dependent on the redox potential of the hole-transport material.

Summary and Conclusions

We have developed an efficient protocol for the synthesis of a variety of soluble hole-transporting polymers which have compact nonfunctionalized backbones and

(23) Estimates of solid-state LUMO levels for different TPD derivatives have been presented at the 214th ACS meeting: Thayumanavan, S.; Barlow, S.; Marder, S. R.; Lee, P.; Anderson, J. D.; Armstrong, N. R.; Jabbour, G. E.: Kawabe, Y.; Morrell, M. M.; Shaheen, S. E.; Kippelen, B.; Peyghambarian, N. *ACS Meeting Abstr.***1997**, 214.

(24) Okutsu, S.; Onikubo, T.; Tamano, M.; Enokida, T. *IEEE Trans. Electron Devices* **1997**, *44*, 1302.

high glass transition temperatures. We have synthesized several hole-transport materials with differences in their redox potential, and we have investigated the effect of the redox potential on the performance of a two-layer LED. The device performance has been found to depend on the redox potential of the hole-transporting material, as illustrated in Figure 7.

This study shows that very electron-rich HTL materials yield devices with lower external quantum efficiencies. Devices containing HTL materials with a more positive redox potential exhibit higher external quantum efficiencies. This suggests that, providing that hole injection stays in good balance with electron injection in the device, facile hole injection from the anode into the HTL is not crucial for the overall device performance, and improved quantum efficiencies can be achieved through facilitating the redox reactions at the HTL/EL interface. Specifically, we have found that the redox behavior of unsubstituted TPD is not optimal for the ITO/HTL/Alq/Mg LED configuration. Higher quantum efficiencies have been observed for polymers containing TPA and fluoro-TPD (**P4** and **P3**). Finally, device stability was found to depend on the redox potential of the HTL material: more electron-rich derivatives yield devices with improved lifetimes.

Acknowledgment. We thank Prof. Neal R. Armstrong, Dr. Stephen Barlow, Dr. S. Thayumanavan, and Prof. Ghassan E. Jabbour for very helpful discussions and Dr. Steven Barlow and Dr. S. Thayumanavan for providing samples of the molecular TPD derivatives. Financial support was received through the Center of Advanced Multifunctional Nonlinear Optical Polymers and Molecular Assemblies (CAMP) from the Office of Naval Research. NSF-AASERT student support through BMDO-AFOSR is gratefully acknowledged.

CM980614R